

DYNAMICS OF SHEAR HOMEOMORPHISMS OF TORI AND THE BESTVINA–HANDEL ALGORITHM

TALI PINSKY — BRONISŁAW WAJNRYB

ABSTRACT. Sharkovskii proved that the existence of a periodic orbit of period which is not a power of 2 in a one-dimensional dynamical system implies existence of infinitely many periodic orbits. We obtain an analog of Sharkovskii's theorem for periodic orbits of shear homeomorphisms of the torus. This is done by obtaining a dynamical order relation on the set of simple orbits and simple pairs. We then use this order relation for a global analysis of a quantum chaotic physical system called the kicked accelerated particle.

1. Introduction

Given a dynamical system (X, f) , a key question is which periodic orbits exist for this system. Since periodic orbits are in general difficult to compute, we would like to have the means to deduce their existence without having to actually compute them.

Sharkovskii addressed the dynamics of continuous maps on the real line. He defined an order \triangleleft on the natural numbers, Sharkovskii's order (see [14]), and proved that the existence of a periodic orbit of a certain period p implies the existence of an orbit of any period $q \triangleleft p$. We say the q orbit is *forced* by the p orbit. This offers the means of showing the existence of many orbits if one can find a single orbit of "large" period. For a dynamical system depending

2010 *Mathematics Subject Classification.* 37E30, 37E40, 37E45.

Key words and phrases. Torus homeomorphisms, dynamical systems, forcing, periodic orbits.

on a single parameter, if periodic orbits appear when we change the parameter, they must appear according to the Sharkovskii's order. Hence, Sharkovskii's theorem gives the global structure of the appearance of periodic orbits for one dimensional systems. Ever since the eighties there has been interest in obtaining analogs for Sharkovskii's theorem for two dimensional systems (see [4] and [16]).

A homeomorphism of a torus is said here to be of *shear type* if it is isotopic to one Dehn twist along a single closed curve. Let h be a shear homeomorphism, and let x be a periodic orbit of h . We can then define the *rotation number* of x , see discussion in Section 2. Thus, a rational number in the unit interval $[0, 1)$ is associated to each orbit.

We consider orbits up to conjugation: orbits (x, f) and (y, g) are *similar* (of the same type) if there exists a homeomorphism h of the torus T^2 such that h is isotopic to the identity, h takes orbit x onto orbit y and hfh^{-1} is isotopic to g rel y . We define below a specific family of periodic orbits we call simple orbits. In this family there is a unique element up to similarity corresponding to each rotation number; hence they can be specified by their rotation numbers. We emphasize it is not true in general that an orbit of a shear homeomorphism is characterized by its rotation number.

Simple orbits are analyzed in Section 2. As it turns out (see Remark in Section 2), one simple orbit is indeed simple and does not force the existence of any other orbit. More generally a periodic orbit is of *twist type* if it does not force the existence of any orbit of different type with the same rotation number. It is tempting to conjecture that the simple orbits are the only orbits of twist type, but Lemma 2.4 shows that this is false. We give there an example of an orbit of twist type which is not simple. This example also shows that a periodic orbit with a given rotation number does not necessarily force a simple orbit of the same rotation number.

We turn in Section 3 to analyze pairs of orbits. Two coexisting simple periodic orbits can form a simple pair and these are considered. The pairs do force some more interesting dynamics, as follows. We denote the integers by letters p, q and the rational numbers by r, s, t possibly with indices. For a pair of simple orbits of rotation numbers q_1/p_1 and q_2/p_2 to constitute a simple pair, it is necessary that the rotation numbers be Farey neighbours, i.e. $|p_2q_1 - p_1q_2| = 1$. We denote such a pair of rational numbers by $q_1/p_1 \vee q_2/p_2$.

We now define an order relation on the following set \mathcal{P} of rational numbers and pairs in the unit interval,

$$\mathcal{P} = \{r \mid r \in \mathbb{Q} \cap [0, 1)\} \cup \{r \vee s \mid r, s \in \mathbb{Q} \cap [0, 1)\}.$$

Define the order relation on \mathcal{P} to be

$$r \vee s \succ t \Leftrightarrow t \in [r, s] \quad \text{and} \quad r_1 \vee r_2 \succ s_1 \vee s_2 \Leftrightarrow s_1, s_2 \in [r_1, r_2].$$

where we denote by $[r_1, r_2]$ the interval between r_1 and r_2 , regardless of their order.

THEOREM 1.1. *The order relation \succsim on \mathcal{P} describes the dynamical forcing of simple periodic orbits. Namely, the existence of a simple pair of periodic orbits with rotation numbers $r \vee s$ in \mathcal{P} implies the existence of all simple orbits and simple orbit pairs of rotation numbers smaller than $r \vee s$ according to this order relation.*

This is the main result of this paper and the proof is completed in Section 4. The idea of the proof is as follows. Consider the torus punctured on one or more periodic orbits of a homeomorphism h . Then h induces an action on this punctured torus, and on its (free) fundamental group. Now apply the Bestvina–Handel algorithm to this dynamical system. The idea of using the Bestvina–Handel algorithm was used by Boyland in [6] and he describes the general approach in [5]. In our case, after puncturing out a simple pair of orbits, applying the algorithm yields an isotopic homeomorphism which is pseudo-Anosov. The algorithm also offers a Markov partition for this system and we use the resulting symbolic representation to find that there are periodic orbits of each rotation number between the pair of numbers we started with. Then we directly analyze the structure of the pseudo-Anosov representative to show that all these orbits are in fact simple orbits. Furthermore any two of them corresponding to rotation numbers which are Farey neighbours form a simple pair. Finally we establish the isotopy stability of these orbits using results of Asimov and Franks [2] and Hall [11]. Thus, the orbits exist for any homeomorphism for which the simple pair exists, and are forced by it.

One should compare this result with a very strong theorem of Doeff (see Theorem 3.6), where existence of two periodic orbits of different periods for a given shear homeomorphism h implies existence of periodic orbit of every intermediate rotation number. However an explicit description of these orbits is not given, while our stronger assumptions imply existence of simple periodic orbits and simple pairs of orbits. It may be true that the existence of any two periodic orbits with different rotation numbers implies the existence of a simple orbit with any given intermediate rotation number, but we feel that the evidence is not strong enough to make a conjecture either way, in particular in view of Lemma 2.4. Even more difficult question is to determine whether there exists a simple pair of periodic orbits in the situation of Doeff Theorem. First one should try to find a pair of simple orbits which is not a simple pair while the rotation numbers are Farey neighbours, but it is very difficult to understand the geometry of the pseudo-Anosov homeomorphism which arises in this situation.

This research was originally motivated by a question we were asked by Professor Shmuel Fishman: Is there a topological explanation for the structure of

appearance of accelerator modes in the kicked particle system. In Section 5 we give a description of the kicked particle system. This system turns out to be described precisely by a family of shear homeomorphisms of the torus. The existence of accelerator modes is equivalent to existence of periodic orbits. The global structure of this system is given by the order relation in Theorem 1.1, while it cannot be directly computed due to the complexity of the system.

The authors would like to thank Professor Shmuel Fishman for offering valuable insights, Professor Italo Guannieri for some critical advice, and Professor Philip Boyland for many indispensable conversations.

2. Simple orbits

Let $\{x_1, \dots, x_N\}$ be a set of points belonging to one or more periodic orbits for a homeomorphism f of a surface S . The dynamical properties of this set of orbits are captured by the induced action of f on the complement $S_0 = S \setminus \{x_1, \dots, x_N\}$ in a sense that will shortly become clear. Choose any graph G which is a deformation retract of the punctured surface S_0 . A homeomorphism of S_0 then induces a map on G . The converse is also true: a given map of G determines a homeomorphism of S_0 up to isotopy. Therefore we specify the periodic orbits we analyze in terms of the action on a graph which is a deformation retract of the surface after puncturing out the orbit.

Denote by G_N the graph obtained by attaching N small loops to the standard unit circle at the points $\exp(2\pi j i/N)$, $j = 0, \dots, N - 1$.

DEFINITION 2.1. We call a periodic orbit $x = \{x_1, \dots, x_N\}$ for a shear homeomorphism f on the two-torus a *simple orbit* if the following hold:

(1) There can be found a graph G which is a deformation retract of $T_0 = T^2 \setminus x$ as on Figure 1 such that G is homeomorphic to G_N .

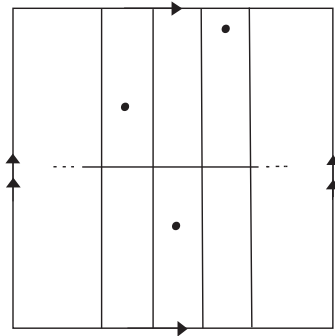


FIGURE 1. A standard graph for a simple orbit.

We call the loop in G corresponding to the unit circle the *horizontal loop* and the loops attached to it the *vertical loops*.

(2) There exists a homeomorphism \tilde{f} of T_0 isotopic to f rel x (i.e. the isotopy is fixed on x) so that a neighbourhood of G is invariant under \tilde{f} and the induced action on G satisfies:

- (a) There exists a fixed number $k \in \{0, \dots, N - 1\}$ such that each vertical loop is mapped k loops forwards (clockwise along the unit circle) to another vertical loop.
- (b) The horizontal loop is mapped to itself with one twist around one of the vertical loops.

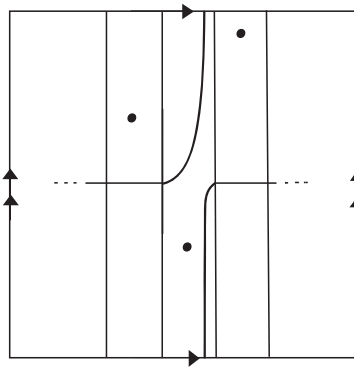


FIGURE 2. The action on a standard graph for a simple orbit.

REMARK 2.2. A homeomorphism h for which we are given a simple periodic orbit must be of shear type as we can deduce from the action on the homology of the non-punctured torus.

For a shear homeomorphism there exists a basis for the first homology for which the induced map is represented by the matrix $\begin{pmatrix} 1 & 0 \\ 1 & 1 \end{pmatrix}$. From here on we refer to any two axes given by an homology basis that gives us the above representation as *standard axes*. The horizontal loop and one of the vertical loops in a graph for a simple orbits constitute a standard basis.

DEFINITION 2.3. Let h be a shear homeomorphism, and let \hat{h} be a lift of h to the universal cover (a plane). For any periodic point x of h of period p , \hat{h}^p maps any lift \hat{x} of x the same integer number q along the horizontal axis away from \hat{x} , in a standard choice of axis (and \hat{x} is possibly mapped some integer number along the vertical axis as well). We can then define the *rotation number* of x to be $\rho(x) = q/p \pmod 1$. The rotation number does not depend on the lift \hat{h} of h .

(The rotation number is often define relative to the given lifting of the homeomorphism h and is not computed modulo 1, but we want it to depend only on the orbit and not on the lifting. In particular we want a simple orbit to have well defined rotation number independent of the lifting of h .)

REMARK 2.4. In the case of a homeomorphism isotopic to a Dehn twist on a torus, which is our interest here, it can be easily shown that the abelian Nielsen type equals exactly the rotation number defined above.

There exists a simple orbit for any given rational rotation number $r \in [0, 1)$, and it is unique up to similarity. Denote the similarity class by \widehat{r} . In the following we use the word vertical to describe the y axis, in a standard choice of axis for f (the direction along which the twist is made).

LEMMA 2.5. *Let x be a periodic orbit for a shear-type homeomorphism f of T^2 for which there exists a family of vertical loops such that they bound a set of annuli each containing one point of the periodic orbit, and this family is invariant under a homeomorphism \widetilde{f} isotopic to f rel x . Then x is a simple orbit.*

PROOF. Choose a vertical loop l of the invariant family. f is orientation preserving, and so is \widetilde{f} . The first loop to the right of l is therefore mapped to the first loop to the right of $\widetilde{f}(l)$. Hence, the vertical loops in the invariant family are all mapped the same number of loops to the right.

Now we have to find a horizontal line with the desired image. We write the invariant family of loops as $\{l_i\}_{i=1}^p$, where $p = \text{period}(x)$, ordered along the horizontal axis. We choose another family of vertical loops $\{m_i\}_{i=1}^p$, such that m_i is contained in the annulus between l_i and l_{i+1} ($l_{p+1} = l_1$), and passes through the periodic point x_i also contained in this annulus. Choose a point $a_1 \neq x_1$ on m_1 . f can be adjusted in such a way that the new homeomorphism \widetilde{f} leaves both families of vertical loops invariant, and in addition, so that a_1 be a periodic point of \widetilde{f} with period p . We denote the orbit of a_1 by $\{a_i\}_{i=1}^p$ where $a_i \in m_i$ for $1 \leq i \leq p$.

Choose a line segment n_1 connecting a_1 to a_2 , so it crosses the annulus between m_1 and m_2 from side to side. We choose n_{j+1} to be the line segment $\widetilde{f}^j(n_1)$ for $1 \leq j \leq p-2$. The boundary points of n_j and n_k coincide whenever they lie on the same vertical loop.

Now, we look at the horizontal loop $n = \bigcup_{j=1}^p n_j$. Each segment of n is mapped exactly to the next segment, except n_{p-1} which is mapped into the annulus between m_1 and m_2 . Since the mapping class group of an annulus is generated by a twist with respect to any loop going once around the annulus we may assume, that n_p is mapped to n_1 plus a number of twists along such a loop. On the other hand we know that $f(n)$ is homotopic to itself plus one twist in the negative direction (on the closed torus), so \widetilde{f} maps n to itself plus one negative twist along this loop. By further adjustment of \widetilde{f} we may assume the twist is made along l_2 . Thus the union of the vertical family $\{l_i\}$ with n chosen as above constitute a graph showing x to be a simple orbit. \square

The Thurston–Nielsen classification theorem, see [7], states that any homeomorphism f on a closed connected oriented surface of negative Euler characteristic is isotopic to a homeomorphism \tilde{f} which is

- pseudo Anosov, or
- of finite order, or
- reducible,

where a homeomorphism ϕ is called *of finite order* if there exists a natural number n such that $\phi^n = id$. A homeomorphism ϕ is called *pseudo-Anosov* if there exists a real number $\lambda > 0$ and a pair of transverse measured foliations (\mathcal{F}^u, μ^u) and (\mathcal{F}^s, μ^s) with $\phi(\mathcal{F}^u, \mu^u) = (\mathcal{F}^u, \lambda\mu^u)$ and $\phi(\mathcal{F}^s, \mu^s) = (\mathcal{F}^s, (1/\lambda)\mu^s)$. A homeomorphism ϕ on a surface M is called *reducible* if there exists a collection of pairwise disjoint simple closed curves $\Gamma = \{\Gamma_1, \dots, \Gamma_k\}$ in $\text{int}(M)$ such that $\phi(\Gamma) = \Gamma$ and each component of $M \setminus \Gamma$ has a negative Euler characteristic. The representative \tilde{f} in the isotopy class of f which is of one of the three forms above is called the Thurston–Nielsen canonical form of f .

When the surface has a finite number of punctures and ϕ permutes the punctures then the same is true except that in the case of pseudo-Anosov map we treat the punctures as distinguished points (there is a unique way to extend a homeomorphism to the distinguished points) and we allow an additional type of singularities of the measured foliations, the 1-prong singularities at the distinguished points (see [11], and Section 0.2 of [3]).

Of course homeomorphism f is reducible with respect to a simple orbit since it contains an invariant family of loops $\{l_i\}$ and the complement of the invariant family consists of punctured annuli (which have negative Euler characteristic).

REMARK 2.6. A homeomorphism f with a simple orbit x can be constructed in such a way that x is the only periodic orbit of f . The invariant set of vertical loops is evenly spaced with the distance between the consecutive loops equal to $1/p$. The loops are moved by q/p to the right and by fixed irrational number downward. Punctures (the points of the periodic orbit) are also evenly spaced and have the same height. The vertical lines containing punctures are moved by q/p to the right. The punctures keep their height and all other points of the loop move a little downwards. Every other vertical line is moved to another vertical line by a little more than q/p to the right (not all lines by the same distance).

EXAMPLE 2.7. Not every periodic orbit for a shear homeomorphism is reducible. Consider the homeomorphism h described on Figure 3. It takes the graph on the left of Figure 3 to the graph on the right and is a shear homeomorphism. It has a periodic orbit of order 2, shown on the pictures, with rotation number $1/2$ and it is pseudo-Anosov in the complement of the orbit.

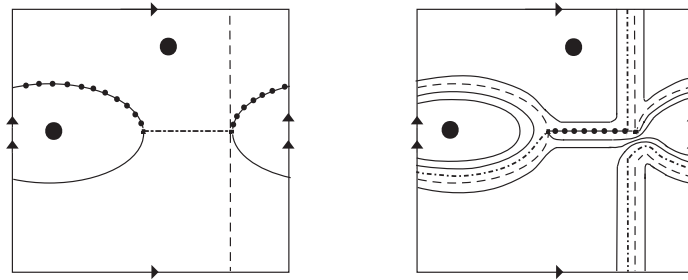
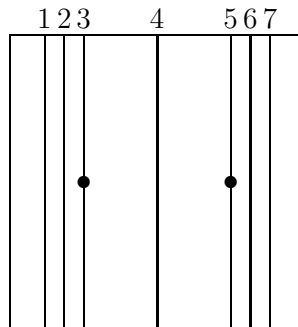


FIGURE 3

LEMMA 2.8. *There exists an orbit of twist type for a shear homeomorphism of the torus which is not simple.*

PROOF. We construct an example of an orbit of length 4 with the rotation number $1/2$. It cannot be a simple orbit and yet we prove it does not force the existence of any periodic orbit not similar to itself, and is thus of twist type. Such examples may be known, possibly considered for a different phenomena. We include it here in order to show the independence of our results.

FIGURE 4. Some vertical lines in U_2 .

We represent the torus as the unit square with the opposite sides identified. The points A_1, \dots, A_4 of the orbit are spaced evenly on the horizontal middle line with the x -coordinate $1/8, 3/8, 5/8, 7/8$. We split the square into 2 equal parts U_1 and U_2 by the vertical line $x = 1/2$. Homeomorphism h translates U_1 to the right to U_2 . Vertical lines go to vertical lines, lines $x = 0$ and $x = 1/2$ move downward by an irrational number $\alpha < 1/40$ and the movement is damped out to the horizontal translation for $t < \alpha$ and $t > 1/2 - \alpha$, so the other vertical lines are translated horizontally by $1/2$. In particular A_1 moves to A_3 and A_2 moves to A_4 .

The restriction of h to U_2 is defined in two steps. The second step simply translates U_2 horizontally by $1/2$ to the right (which is the same as the translation

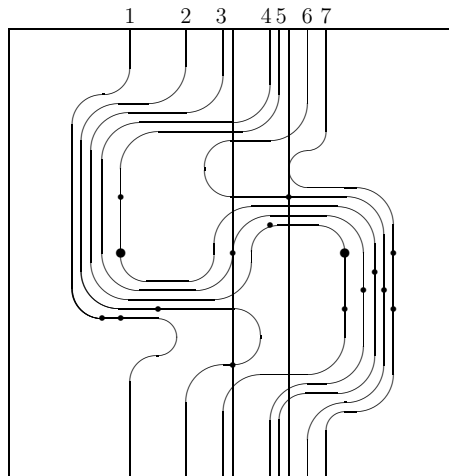


FIGURE 5. The foliation in U_2 realizing a non-simple orbit of twist type.

by $1/2$ to the left). The first step is isotopic to the half-twist along the segment connecting A_3 and A_4 , followed by the Dehn twist with respect to the right side (right boundary of the cylinder). In particular it switches A_3 and A_4 . We shall prove that we can construct such h for which h^2 has no fixed points and therefore h has no periodic orbit of length 2 and in particular no simple orbit with the rotation number $1/2$.

We describe the first step of h restricted to U_2 . Figure 4 shows some vertical lines in U_2 , the big dots show the points A_3 and A_4 of the periodic orbit. Figure 5 shows their images under the first step. In these pictures U_2 is represented as a square, to make more space, but in the reality the base has length $1/2$ and the height is equal to 1. Line $x = 1/2$ is mapped to itself and moves downward by α . The near by vertical lines (for $t < 1/2 + 1/30$) are moved to the vertical lines and to the right where line $x = 1/2 + 1/30$ is moved to the line $x = 1/2 + 1/20$. For $t \in (1/2 + 1/30, 1 - 1/20)$ the line $x = t$ is moved to a curve L_t and for $t \in (1 - 1/20, 1)$ the line $x = t$ moves to a vertical line to the right of it and downward, to get the full Dehn twist plus a movement downward by α when we get to the line $x = 1$. For $t \in (1/2 + 1/30, 1 - 1/20)$ curve L_t starts at a point on the top side to the right of $x = t$, it moves to the left, then to the right, then to the left again and ends at the bottom side (exactly below its starting point). In particular each vertical line meets L_t in at most two points. Some lines L_t are shown on Figure 5.

We may arrange it in such a way that there exist t_0, t_1 such that $1/2 < t_0 < t_1 < 1$ and the line $x = t$:

- is disjoint from L_t , and lies on the left side of L_t when $t < t_0$;
- meets L_t at one point for $t = t_0$;

- meets L_t at two points when $t_0 < t < t_1$;
- meets L_t at one point for $t = t_1$;
- is disjoint from L_t and lies on the left side of L_t when $t_1 < t < 1$.

We get a new trivial foliation of the annulus U_2 . In step 1 we map the vertical foliation onto the new foliation L_t . We can further change the first step moving each leave L_t along itself to reach the following goal. Let P_t, Q_t denote the intersection points of $x = t$ with L_t , P_t lies below Q_t (the points coincide for t_0 and t_1). For $t = t_0$ the line $x = t$ meets L_t in one point P_t . We may assume that the image of P_t in L_t lies in the part below P_t . Then for the nearby leaves the images of both points P_t and Q_t lie in the lower part of L_t below the point P_t (see the small dots on the first curve in Figure 5). The images of P_t and Q_t lie further away from each other when we move to the right (see the small dots on the second curve). The third line passes through A_3 , its image L_t passes through A_4 and the images of P_t and Q_t lie on different sides of A_4 along the third curve. Next the upper point Q_t moves backwards along L_t and when we reach the fourth line of Figure 4 (also shown on Figure 5) it coincides with the point P_t on L_t . Next the image of Q_t lies inside the arc of L_t between the points P_t and Q_t and when we reach the fifth line on Figure 4, which passes through the point A_4 , then the curve L_t passes through A_3 and the image of Q_t on L_t lies above A_3 (see Figure 5). When we move further to the right the image of the point Q_t moves again forward towards the image of P_t and at the line number 6 on Figure 4 the image of Q_t again coincides with P_t at the intersection of $x = t$ with L_t . Next the images of P_t and Q_t move further down and gets close together and when $t = t_1$ we have one intersection point P_t and its image lie below P_t along L_t . Step 1 has no fixed points. Step 2 translates U_2 to U_1 .

We now consider the homeomorphism h^2 . We start with U_1 . Any point on $x = 0$ and $x = 1/2$ moves down by 2α . Any point with $x \in [0, 1/30]$ moves to a point with a bigger x -coordinate. Any point with $x \in [1/30, 9/20]$ moves horizontally by $1/2$ then we apply step 1, which has no fixed points, and then the point moves again horizontally by $1/2$ so it comes to a new point. Any point with $x \in [9/20, 1/2]$ moves to a point with a bigger x -coordinate.

For points in U_2 the situation is similar. Any point with $x \in (1/2, 16/30]$ moves to a point with a bigger x -coordinate. Any point with $x \in [16/30, 19/20]$ moves under the first step to a new point with the x -coordinate in $[11/20, 29/30]$ and then moves horizontally twice by $1/2$. Finally any point with $x \in [19/20, 1]$ moves to a point with a bigger x -coordinate. Homeomorphism h^2 has no fixed points and h has no periodic points of order 2.

We now show that there exists a homeomorphism f isotopic to h in the complement of the orbit A_1, \dots, A_4 , which has only periodic orbits similar to this orbit and periodic orbits of order 2. We consider parts U_1 and U_2 as before.

The restriction of f to U_1 translates it horizontally by $1/2$. In U_2 we choose two circles with center $(3/4, 1/2)$ and radius $1/7$ and $1/6$, respectively. We rotate the interior of the smaller circle by 180 degrees. The rotation is damped out to the identity at the outer circle and the intermediate circles are moving out towards the outer circle. The exterior of the outer circle with $x < 19/20$ is pointwise fixed. The lines with $x > 19/20$ move to the right and down to get the full Dehn twist when we get to the line $x = 1$. The second step of f restricted to U_2 translates it horizontally by $1/2$. Now each point inside the smaller circle, different from its center (which has period 2), belongs to an orbit similar to A_1, \dots, A_4 . Points between the circles and points with $x \in (19/20, 1)$ are not periodic and other points in U_2 have period 2 and the same is true for the corresponding points in U_1 .

Therefore the orbit A_1, \dots, A_4 does not force any periodic orbit not similar to itself. □

3. Simple orbit pairs

Let x and y be two coexisting simple periodic orbits, for a homeomorphism f of T^2 (f must be of shear type), with rotation numbers q_1/p_1 and q_2/p_2 respectively. Assume $p_1 > p_2$, i.e. y has lesser period than x .

DEFINITION 3.1. We call the pair of orbits a *simple pair* if:

- (a) We can find an embedded graph G in their complement homeomorphic to G_{p_1} as on Figure 6.

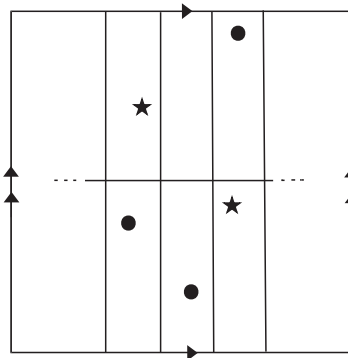


FIGURE 6

Each component in the complement of the graph is a topological rectangle which contains exactly one point of orbit x and at most one point of orbit y .

- (b) The homeomorphism f acts on this graph in the following way: each vertical loop except one moves to another vertical loop, there is one vertical loop

denoted l such that $f(l)$ is a vertical loop m plus a small loop around one point of the (shorter) y orbit, in a rectangle adjacent to line m on the right (as on Figure 7) or on the left, and the horizontal line is mapped to itself plus a twist in the negative direction around $f(l)$, as on Figure 7.

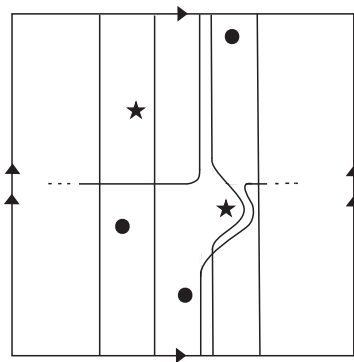


FIGURE 7

The graph which appears in Definition 3.1 divides the torus T^2 into p_1 rectangles. The homeomorphism f moves each vertical loop the same distance, say k rectangles, to the right except for the small additional loop for line l . Let R_0 be the rectangle adjacent to m in which the small loop in the image of the graph occurs. R_0 must contain exactly one point of each orbit. We denote these points x_0 and y_0 respectively. Under p_1 iterations of f the point x_0 runs q_1 times around the whole torus, that is $q_1 p_1$ rectangles to the right. So, $p_1 k = q_1 p_1$ and $k = q_1$.

The point y_0 is mapped to itself after p_2 iterations. Under each iteration the image of y_0 is mapped k ($= q_1$) rectangles to the right, except the last iteration under which it is moved an additional rectangle to the right or left. Altogether it has moved $p_2 q_1 \pm 1$ rectangles. At the same time, it is mapped around the torus q_2 times, hence $q_2 p_1$ rectangles. This means $p_2 q_1 \pm 1 = q_2 p_1$. Thus for a simple pair of periodic orbits the rotation numbers q_1/p_1 and q_2/p_2 are Farey neighbours and the additional loop is on the right (as on Figure 7) if and only if $q_2/p_2 > q_1/p_1$. Denote by $\widehat{r} \vee \widehat{s}$ the similarity class of a simple pair corresponding to a pair of Farey neighbours $r \vee s$.

Consider again the points x_0 and y_0 in the rectangle R_0 . Continue the notation to all the points of x and y by $x_i = f^i(x_0)$ and $y_i = f^i(y_0)$. We draw a small loop around each of the points of y . The union of these loops will be the peripheral subgraph P for the Bestvina–Handel algorithm, since we may assume the union of these loops to be f -invariant. Now we consider separately two cases. Case 1 will be the case in which m is the left boundary curve of R_0 , while in

case 2 it is the right boundary (in other words in the first case $q_1/p_1 < q_2/p_2$ and in the second case $q_1/p_1 > q_2/p_2$). Choose some point on the loop around y_0 and connect it, by a curve l_0 , to a point on the section of the horizontal line in R_0 , in case 1 from below the segment and in case 2 from above.

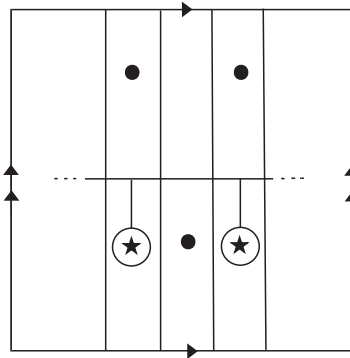


FIGURE 8

Then $f(l_0)$ is a curve connecting the loop around y_1 and the corresponding horizontal segment. We denote it by l_1 , and do the same for each y_i . After adding the above edges to the graph case 1 is topologically as in Figure 8.

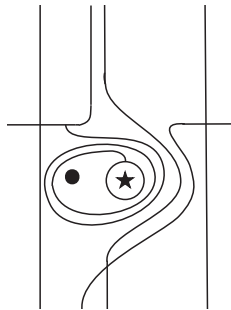


FIGURE 9

The inclusion $G \hookrightarrow S_0$ is a homotopy equivalence (where S_0 is the punctured torus). We know the action of f on all edges of G except for the curve l_{q_1-1} connecting y_{q_1-1} and the horizontal segment in the corresponding rectangle. It's image is a curve connecting the horizontal segment in the rectangle adjacent to m which is not R_0 to the loop around y_0 . This image might wind around a disk containing y_0 and x_{q_1-1} as in Figure 9.

The graph and its image for case 2 are exactly the same except that the loops are connected to the horizontal segments from above. We shall prove in

Proposition 3.2 that we may assume that the image of the segment l_{q_1-1} has no winding. Hence we draw from now on the graph images without winding, and we may assume that the graphs given in Figure 10 also have an invariant neighbourhood by a further isotopy of f .

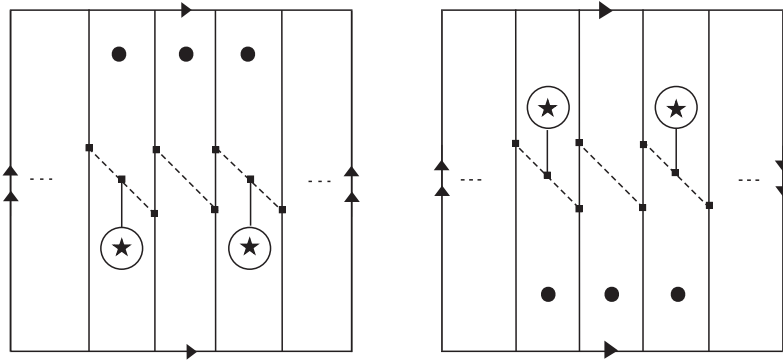


FIGURE 10. The standard graph for a simple pair, case 1 on the left and case 2 on the right.

The action of f (up to isotopy) on this graph is given by one of the actions on Figure 11, drawn in some regular neighbourhood of the graph, where each vertical loop moves q_1 loops to the right.

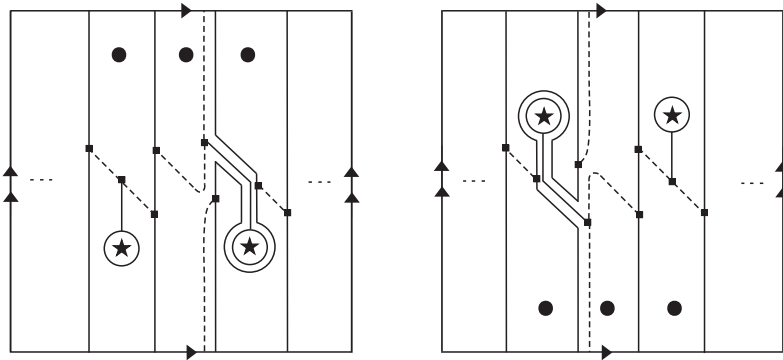


FIGURE 11. The action on a standard graph for a simple pair, for both cases respectively.

PROPOSITION 3.2. *Let $\{x, y\}$ be a simple pair with the graph as on Figure 8 and with windings as on Figure 9. Then there may be chosen a different invariant graph, which also makes $\{x, y\}$ a simple pair, whose image is without winding.*

PROOF. To simplify the picture we prove the proposition for rotation numbers $1/3$ and $1/2$. The general proof proceeds in the same way. We start by

looking at a simple pair $\{x, y\}$ of rotation numbers $1/3$ and $1/2$ for a homeomorphism f with the corresponding invariant graph G given so that the action on it is without any twists, as on the left side of Figures 10 and 11. We now choose a different system of curves (a different graph), in a small neighbourhood of G as in Figure 12, which will serve as a new graph for the pair.

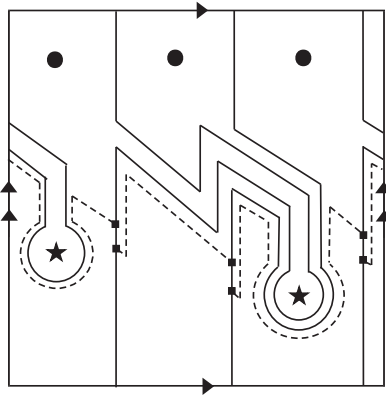


FIGURE 12

Solid lines are the new vertical loops and dashed lines are the new diagonal segments like in Figure 10. The horizontal loop consists of the dashed lines and the long pieces of the solid lines. To move from left to right along the horizontal line, move along a dashed line and turn to the left when meeting a solid line. Continue up along a vertical loop and then along the next dashed line. We add to this graph the peripheral subgraph and the connecting segments and get the graph H as on Figure 13. It is clear that topologically the graph H has the same form as the graph on Figure 10 and that it has an invariant neighbourhood.

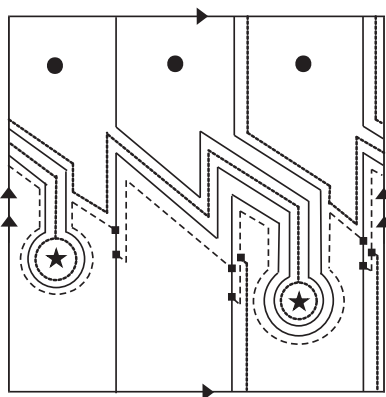


FIGURE 13

The reader can check (using the precise knowledge of the image of each edge of the original graph) that the action of f on the graph H has the properties required from a simple pair. Each vertical loop is mapped onto another vertical loop except for one loop l for which $f(l)$ is equal to a loop m plus a loop around the next periodic point y_p of the shorter orbit. The horizontal loop is mapped onto itself plus a negative Dehn twist along $f(l)$. Consider the image s of the segment which connects the horizontal loop to the periodic point y_{p-1} . When the action has no twist then s moves along the horizontal loop in its positive direction until it meets the original segment connecting to y_p and then it follows along the segment. However in our case s goes first backwards along the horizontal loop than moves in the counterclockwise direction along the boundary of the “rectangle” adjacent to the vertical loop m and finally follows the horizontal loop and the segment to y_p . This means that the action f on the graph H has one positive twist.

We proved that a simple pair for a shear homeomorphism with a given graph and a given action without twists can be given another graph which also describes it as a simple pair and the action on the new graph has one positive twist. This process is reversible. Therefore, by induction, we can add or remove any number of twists using a suitable graph. This implies Proposition 3.2. \square

Hence for a simple pair the action on a spine is given by Figures 10 and 11. We can now apply the Bestvina–Handel algorithm (see [3]), endowing a neighbourhood of G with a fibered structure in the natural way. The algorithm specifies a finite number of steps which we apply to the graph G , altering G together with the induced action on it, but without changing the isotopy class of f on $T^2 \setminus (x \cup y)$. When the algorithm terminates, it gives a new homeomorphism \tilde{f} which is the Thurston Nielsen canonical form of f .

For simple pairs, the action in each of the two cases above is easily seen to be tight, as no edge backtracks and for every vertex there are two edges whose images emanate in different directions. The action has no invariant non-trivial forest or nontrivial invariant subgraph and the graphs have no valence 1 or 2 vertices. This is the definition in [3] for an irreducible map on a graph.

DEFINITION 3.3. Assuming g , the induced map on the graph itself, does not collapse any edges, there is an induced map Dg , the *derivative* of g , defined on

$$\mathcal{L} := \coprod \{(v, e) \mid v \text{ is a vertex of } G, e \text{ is an oriented edge emanating from } v\}$$

by $Dg(v, a) = (g(v), b)$ where b is the first edge in the edge path $g(a)$ which emanates from $g(v)$.

DEFINITION 3.4. We say two elements (v, a) and (v, b) in \mathcal{L} corresponding to the same vertex v are *equivalent* if they are mapped to the same element under $D(g^n)$ for some natural n . The equivalence classes are called *gates*.

The gates in each of the cases above are given by Figure 14, indicated there by small arcs.

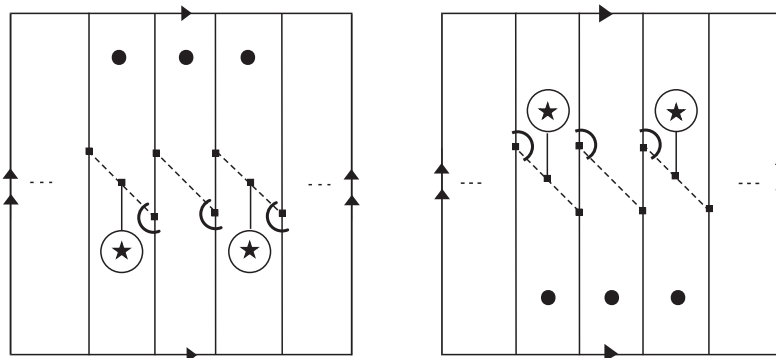


FIGURE 14

There is no edge which g sends to an edge path which passes through one of the gates – enters the junction through one arm of the gate and exits through the other. Such an irreducible map is efficient. i.e. this is an end point of the algorithm. Now, since there are edges mapped to an edge path longer than one edge, we arrive at our next theorem.

THEOREM 3.5. *A homeomorphism f of the two torus for which a simple pair of periodic orbits exists is isotopic to a pseudo-Anosov homeomorphism relative to this pair of orbits.*

Let f be a shear type homeomorphism of the torus, and fix a lift \tilde{f} of f . Define the *lift rotation number* of a point $x \in \mathbb{T}^2$ to be

$$\rho(x, \tilde{f}) = \lim_{n \rightarrow \infty} \frac{(\tilde{f}^n(\hat{x}) - \hat{x})_1}{n},$$

for any lift \hat{x} of x , when the limit exists, where the subscript 1 denotes the projection to the horizontal axis. Define the *rotation set* $\rho(\tilde{f})$ of \tilde{f} to be the set of accumulation points of

$$\left\{ \frac{(\tilde{f}^n(\hat{x}) - \hat{x})_1}{n} \mid \hat{x} \in \mathbb{R}^2 \text{ and } n \in \mathbb{N} \right\}.$$

Then, the above theorem follows from the following much more general theorem by Doeff, see [9] and [10].

THEOREM 3.6 (Doeff). *Let h be a shear type homeomorphism of \mathbb{T}^2 , and fix a lift \tilde{h} of h . If h has two periodic points x and y with $\rho(x, \tilde{h}) \neq \rho(y, \tilde{h})$ then h is pseudo-Anosov relative to x and y . Furthermore, the closure of the rotation set is a compact interval, and any rational point r in the interior of this interval corresponds to a periodic point $x \in \mathbb{T}^2$ with $\rho(x, \tilde{h}) = r$.*

In particular, Doeff proves existence of two periodic orbits of different rotation numbers implies existence of an orbit for any rational rotation number between these two. But he does not give any characterization of these orbits. Example 2.7 shows two different orbits, both with rotation number equal to $1/2$, one of which is pseudo-Anosov, and the other reducible. Thus the rotation number does not give much information about the orbit and in this sense this theorem does not give a satisfactory dynamical understanding of what is happening in regions of coexistence of orbits. In contrast with Doeff's general theorem, we get results for a very specific family of periodic orbits, but for this family we are able to give exactly the orbits forced by others, as we show in Section 4.

In our case the canonical form \tilde{f} of f we get by applying the Bestvina–Handel algorithm is a pseudo Anosov homeomorphism. When this is the case, the algorithm gives a canonical way of endowing a regular neighbourhood S_0 of G with a rectangle decomposition $\{R_1, \dots, R_N\}$. The decomposition is a Markov partition for the homeomorphism \tilde{f} .

A Markov partition for a dynamical system offers a symbolic representation for the system in the following way. Let Σ_N be the subset of the full N -shift (the set of bi-infinite series on N symbols), where N is the number of rectangles in the decomposition. Let Σ be a subset of Σ_N defined by

$$\Sigma = \{s = (\dots, s_n, s_{n+1}, \dots) : R_{s_n} \cap \tilde{f}^{-1}R_{s_{n+1}} \neq \emptyset\}.$$

On Σ we naturally define a dynamical system with the operator of the right shift denoted by σ , and (Σ, σ) is called the subshift corresponding to the dynamical system. Σ can be completely described by stating which transitions $k \rightarrow m$ for $k, m \in \{1, \dots, N\}$ are *allowed* (i.e. for which k, m , $\tilde{f}^{-1}R_m \cap R_k \neq \emptyset$). See [1] for the definitions and for a proof that in this case we can define a map $\pi: \Sigma \rightarrow S_0$ by

$$\pi: s \mapsto \bigcap_{n=0}^{\infty} \overline{\tilde{f}^n R_{s_{-n}} \cap \dots \cap \tilde{f}^{-n} R_{s_n}}$$

which satisfies the following properties:

- $\pi\sigma = \tilde{f}\pi$,
- π is continuous,
- π is onto.

We take here the set of sequences with the Tichonoff topology. Thus a periodic point in the symbolic dynamical system which is just a periodic sequence corresponds to a periodic point in the original dynamical system.

To obtain the Markov partition in our case as in [3], we thicken the edges of the graph to rectangles. In particular, the rectangles can be glued directly to each other without any junctions. This can be done in a smooth way, endowing S_0 with a compact metric space structure by giving a length and width to each rectangle, consistently. Each edge of the standard graph for the pair (Figure 10) corresponds to one rectangle, except the edge which is mapped to the loop around y_0 . This edge we divide in two (this is necessary to avoid having a rectangle intersecting twice an inverse image of another rectangle). Now we have edges of seven different types on the graph. The vertical loops of the graph consist of long edges we denote as A edges, and short edges we call B edges. The loops around the points of the y orbit and vertical segments connecting the loops to the diagonal edges we call C 's and D 's, respectively. In rectangles which contain two punctures and therefore two diagonal edges we call the upper ones L edges and the lower ones K edges in the first case, and the lower ones L edges, upper ones K edges, in the second case. The last type of edges are diagonals of once punctured rectangles, these we call M edges.

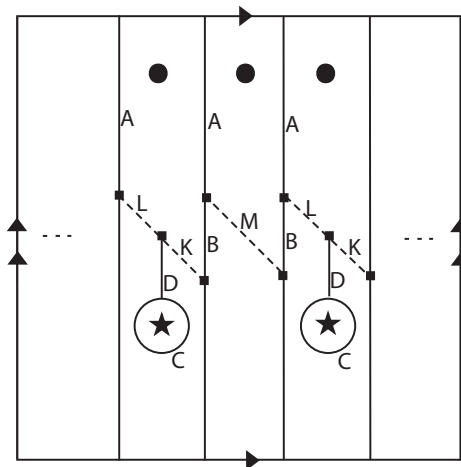


FIGURE 15

Next, we label the rectangles in order to have explicitly the transition rules:

- For $0 \leq i \leq p_2 - 1$ denote the rectangle corresponding to the D edge connecting the loop around y_i to the diagonal by r_{i+1} . Denote the rectangle corresponding to the C edge which is the loop around y_i by r_{p_2+i+1} .

- For $1 \leq i \leq p_2$, denote the rectangles corresponding to the L and K edges connected to r_i by r_{2p_2+i} and r_{3p_2+i} , respectively.
- Denote the rectangle corresponding to the A edge belonging to the vertical line we referred to as m by r_{4p_2+1} and the B edge which is part of the same line m as $r_{4p_2+p_1+1}$.
- For the vertical line $f^i(m)$ denote it's A and B rectangles by r_{4p_2+1+i} and $r_{4p_2+p_1+1+i}$, respectively, for all $1 \leq i \leq p_1 - 2$.
- For the vertical line $f^{p_1-1}(m)$, denote it's A edge as by $r_{4p_2+p_1}$. There are two rectangles corresponding to the B edge as explained above, denote the lower one by $r_{4p_2+2p_1}$ and the upper one by $r_{4p_2+2p_1+1}$.
- Label the $p_1 - p_2$ remaining rectangles corresponding to the M edges by starting with the first of these to the right of m , and then continuing by the order along the horizontal axis, denoting them by $r_{4p_2+2p_1+2}, \dots, r_{3p_1+3p_2+1}$.

Finally, we can look at the diagram in Figure 16, showing the set of rectangles and transitions in this Markov partition which we now use.

A periodic symbolic sequence of allowed transitions gives as explained a periodic point in the original dynamical system. Therefore by this diagram we can easily find other periodic orbits on the torus that must exist for f . We will later prove that these orbits are in fact simple, but this will require some more work. Hence, by this diagram we prove only existence of orbits with specified rotation numbers. For every pair (n, m) of natural numbers, $n, m \neq 0$, by starting from $r_{p_1+4p_2+1}$, going n times around the first loop in the diagram $\{r_{p_1+4p_2+1}, \dots, r_{2p_1+4p_2}\}$, then going $m - 1$ times around the second loop $\{r_1, \dots, r_{p_2}\}$ (and skipping it if $m = 1$) and then returning through the final sequence $\{r_{2p_2+1}, \dots, r_{3p_2}\}$ to $r_{p_1+4p_2+1}$, we get a periodic symbolic allowed sequence, and so a new periodic orbit we denote $O_{n,m}$. These symbolic sequences are all different and hence so are the periodic orbits. We look at a point $p \in O_{n,m}$ such that p is in the rectangle $r_{p_1+4p_2+1}$. For the first $n \cdot p_1$ iterations of p , corresponding to each time the upper loop in the diagram appears in the symbolic sequence of p , the images are contained in the B edges. The vertical loops are mapped under f retaining the same “horizontal distance” from the periodic points from the x orbit to their left. So, p is mapped a total distance of $n \cdot q_1$ along the horizontal axis under $f^{n \cdot p_1}$.

Similarly, point $f^{n \cdot p_1}(p)$, which lies in the rectangle r_1 corresponding to D edge, is mapped a distance q_2 along the horizontal axis under each iteration of f^{p_2} , for every occurrence of the second loop in the symbolic sequence of p . This is because the D edges retain their distance from the y orbit points below them. The final sequence in the symbolic representation of p until the return to the first loop also corresponds to the horizontal distance q_1 . These last points of

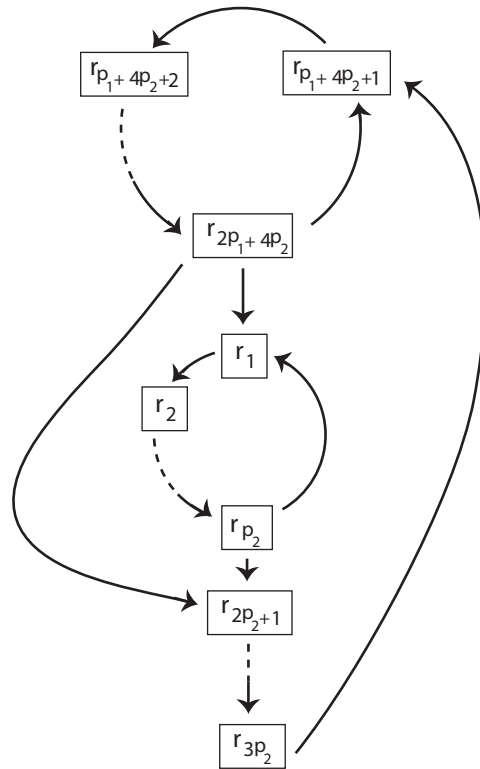


FIGURE 16. Some of the rectangles in the Markov partition, where the arrows denote allowed transitions between them.

the periodic orbit lie in rectangles corresponding to L edges. So p is mapped a horizontal distance of $nq_1 + mq_2$ under $f^{np_1+mp_2}$. Hence, the new orbit $O_{n,m}$ has rotation number $(nq_1 + mq_2)/(np_1 + mp_2)$.

See [12] for a proof that any two Farey neighbours span this way all rational numbers between them, that is all rationals between q_1/p_1 and q_2/p_2 are of the form $(nq_1 + mq_2)/(np_1 + mp_2)$. So we found a periodic orbit of any rational number between the two original rotation numbers q_1/p_1 and q_2/p_2 .

Note we have found these simple periodic orbits for the Thurston–Nielsen canonical form of the homeomorphism f we started with. It remains to relate these periodic orbits to the periodic orbits of f itself. Recall the following definition from [2].

A periodic point $x_0 \in S$ of period p for homeomorphism f_0 is called *unremovable* if for each given homomorphism f_1 with $f_t: f_0 \simeq f_1$ there is a periodic

point x_1 of period p for f_1 and an arc $\gamma: [0, 1] \rightarrow S$ with $\gamma(0) = x_0$, $\gamma(1) = x_1$ and $\gamma(t)$ is a periodic point of period p for f_t .

It was proven by Asimov and Franks in [2] that every periodic orbit of a pseudo-Anosov diffeomorphism is unremovable. Thus orbits found for the pseudo-Anosov representative exist for any other homeomorphism in its isotopy class. This yields all these periodic orbits exist for the original homeomorphism f as well. Thus we get Theorem 3.6 for our specific case:

THEOREM 3.7. *If there exists a simple pair of orbits for a homeomorphism f of the torus of abelian Nielsen types s and t which are Farey neighbours, there exists a periodic orbit for f with abelian Nielsen type equal to r for every rational number r between s and t .*

4. The order relation

For any simple pair $\widehat{q_1/p_1} \vee \widehat{q_2/p_2}$, the orbit $O_{1,1}$ out of the family of new orbits we constructed above has rotation number equal exactly to $(q_1 + q_2)/(p_1 + p_2)$. This orbit corresponds to the symbolic sequence $r_{p_1+4p_2+1} \rightarrow r_{p_1+4p_2+2} \rightarrow \dots \rightarrow r_{2p_1+4p_2} \rightarrow r_{2p_2+1} \rightarrow \dots \rightarrow r_{3p_2} \rightarrow r_{p_1+4p_2+1}$ as in the diagram in Figure 16. So we have a list of rectangles, each containing exactly one periodic point from the new orbit $O_{1,1}$. We denote the point of $O_{1,1}$ that lies in the rectangle r_j by o_j . Graphically, assuming the first case map, when we draw the rectangle decomposition corresponding to the standard graph as in Figure 10 we get Figure 17.

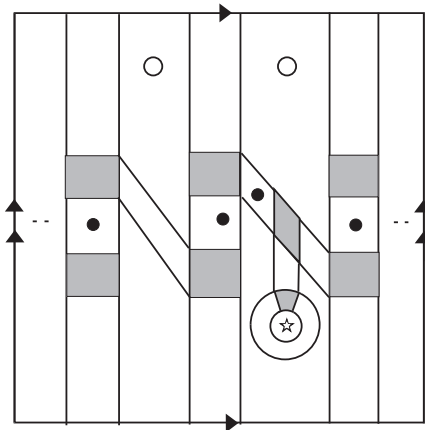


FIGURE 17. The intermediate orbit denoted by black circles. The gray areas are junction, which can be deleted, and the rectangles can be glued directly to one another.

We will now show that for any simple pair $\widehat{q_1/p_1} \vee \widehat{q_2/p_2}$ the orbit $O_{1,1}$ is a simple orbit, and forms a simple pair with each periodic orbit of the pair, that is

$p_2q_1 = p_1q_2 - 1$ rectangles to the right, which means one rectangle to the left of line m . Since A and B are to the right of the point $o_{p_1+4p_2+1}$ in line m and since this point moves to the leftmost point in the new periodic orbit shown on Figure 18, loop C must be to the right of it, as in Figure 18. The point o_{2p_1+1} may be above or below the loop C but this does not change the discussion below.

Note that if we disregard the orbits x and y of the original pair we can isotop C to A relative the points of the new orbit. This shows that the new orbit is a simple periodic orbit of length $p_1 + p_2$, by Lemma 2.5. Now we fill in the x orbit (the longer orbit) and consider a torus punctured at the y orbit and the new orbit together. We have the family of vertical loops $f^i(A)$ and the action on it is exactly as in the condition for a simple pair as the loop C can be isotoped to A plus a loop around y_0 . We choose a horizontal loop as the loop D on Figure 19. Then its image D' is as shown on Figure 19. The image has the required properties. The orbit y together with the new orbit form a simple pair for the homeomorphism f .

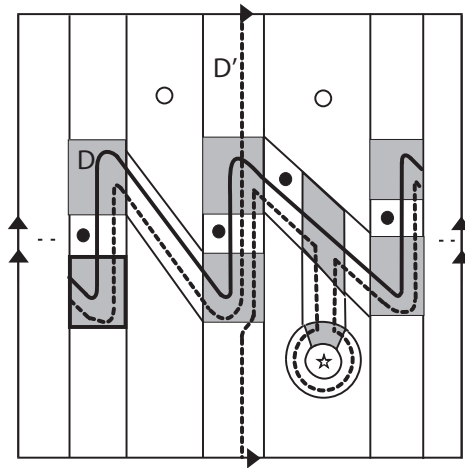


FIGURE 19

Next we fill in the y orbit and leave punctures at the x orbit and the new orbit. We choose the initial vertical loop A differently, as in Figure 20. This loop A is one rectangle to the right of m plus a loop on the left. After $k = p_2 - 1$ iterations of f it will move to line l which is q_1 rectangles to the left of m . Indeed it will move to $q_1(p_2 - 1) + 1 = p_1q_2 - q_1$ rectangles to the right of m which means q_1 rectangles to the left. The loop $f^k(A)$ looks like the loop A and lies to the left of the point r_{3p_2} and to the left of the point $o_{2p_1+4p_2}$. Next iteration of f takes it to a curve which looks like $f(l)$ but lies to the left of $o_{p_1+4p_2+1}$ and to the left of o_{2p_2+1} . Since we filled the point y_0 we can isotop this loop to a vertical loop

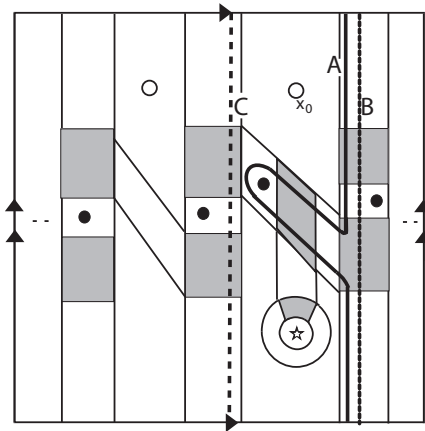


FIGURE 20

near m , which passes to the left of $o_{p_1+4p_2+1}$. Subsequent iterations translate it to the right and $f^{p_1}(A)$ is equal to curve B on Figure 20.

Next $p_2 - 1$ iterations will take B to the loop near l which lies to the left of $o_{2p_1+4p_2}$. Next iteration of f takes this loop to a loop similar to $f(l)$, but lies to the left of o_{2p_2+1} . Since the points of y -orbit are filled we can isotop it to the loop C on Figure 20. It can be further isotoped, relative to the x -orbit and the new orbit, to the loop A plus a small loop around x_0 to the left of A . If we choose the same horizontal loop as in the previous case, with the same image as before, we get the required action of f for a simple pair consisting of the x -orbit and the new orbit.

Now we can continue by the same analysis for each of these two simple pairs, finding their Farey intermediate to be a simple orbit as well that forms a simple pair with each of them, and so on. It remains to prove the persistence of all these simple pairs under isotopies. For this, recall the following theorem from [11].

THEOREM 4.1 (Hall). *Let S be a closed surface and let A be a finite subset of S . Let f be a homeomorphism of S which leaves A invariant. Let $\mathbf{p} = x_1, \dots, x_k$ be a finite collection of periodic points for f which are essential, uncollapsible, mutually non-equivalent and non-equivalent to points of A . Then the collection \mathbf{p} is unremovable, which means that for every homeomorphism g isotopic to f rel A there exists an isotopy f_t rel A and paths $x_i(t)$ in S such that $f_0 = f$, $f_1 = g$, $x_i(0) = x_i$, $x_i(t)$ is a periodic point of f_t of period equal exactly to the period of x_i .*

(This theorem is a generalization of the main result of Asimov and Franks in [2] to several periodic orbits. In fact this generalization was mentioned in [2] as a remark with a hint of a proof.)

Recall also that if f is pseudo-Anosov in the complement of A then it is condensed and by [6] Lemma 1 and Theorem 2.4 each periodic point is uncollapsible and essential and points from different orbits are non-equivalent and points disjoint from A are not equivalent to points of A .

COROLLARY 4.2. *Let T be a torus and let A be a finite subset of T . Let f be a shear-type homeomorphism of T which is pseudo-Anosov in the complement of A . Let g be a homeomorphism of T isotopic to f in the complement of A . If x is a simple periodic orbit for f then there exists a simple periodic orbit z for g with $\rho(z) = \rho(x)$. If x, y is a simple pair of periodic orbits for f , one or both disjoint from A , then there exists a simple pair of periodic orbits z, w for g with $\rho(z) = \rho(x)$ and $\rho(w) = \rho(y)$.*

PROOF. Choose points x_1 and y_1 from the orbits x and y . By Theorem 4.1 there exists an isotopy f_t and paths $x_1(t)$ and $y_1(t)$ such that $x_1(0) = x_1, y_1(0) = y_1, x_1(t)$ is a periodic point of f_t of a fixed order p for all t and $y_1(t)$ is a periodic point of f_t of a fixed order q for all t and $y_1(t) = y_1(0)$ for all t if $y(0) \in A$. For a given t all points in the orbits of $x_1(t)$ and $y_1(t)$ for f are distinct, they form a braid with $p + q$ strands. They move when t changes and their movement can be extended to an ambient isotopy h_t which is fixed on A . Then $h_t(f^i(x_1(0))) = f_t^i(x_1(0))$ and $h_t(f^i(y_1(0))) = f_t^i(y_1(0))$. Consider isotopy $F_t = h_t^{-1}f_t h_t$. We have $F_t(f^i(x_1(0))) = f^{i+1}(x_1(0))$ and $F_t(f^i(y_1(0))) = f^{i+1}(y_1(0))$ so F_t is fixed on the orbits x and y . In particular x and y form a simple pair of periodic orbits for F_1 (or x forms a simple periodic orbit for F_1 if there is no y). But $F_1 = h_1^{-1}gh_1$ so $h_1(x)$ and $h_1(y)$ form a simple pair of periodic orbits for g . \square

This concludes the proof of Theorem 1.1.

5. Global analysis of the kicked accelerated particle system

The physical system called the kicked accelerated particle consists of particles that do not interact with one another. They are subject to gravitation and so fall downwards, and are kicked by an electro-magnetic field, i.e. the electro magnetic field is turned on for a very short time once in a fixed time interval. This electromagnetic field is a sine function of the height of the particle, hence the particles are kicked upwards or downwards by different amounts, depending on their position at the time of a kick. For a short review of the results for this system see [8]. Experiments of this system were conducted by the Oxford group, see [17], and the system was found to show a phenomena that is now called “quantum accelerator modes”: as opposed to the natural expectation that particles fall with more or less the gravitational acceleration, it was found that a finite fraction of the particles fall with constant nonzero acceleration relative to gravity, as can be seen in Figure 21.

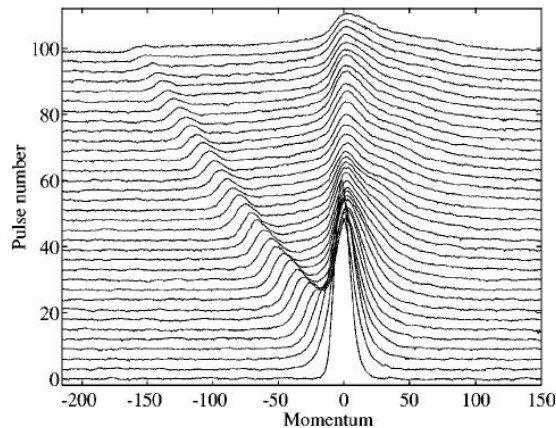


FIGURE 21. Accelerator modes. Experimental data (taken from Oberthaler, Godun, d'Arcy, Summy and Burnett, see [17]) showing the number of atoms with specified momentum relative to the free falling frame as the system develops in time (the numbers on the y axis represents time by the number of kicks, while the z coordinate is proportional to the number of atoms).

This is a truly quantum phenomenon having no counterpart in the classical dynamics. A theoretical explanation for this phenomenon was given by Fishman, Guanieri and Rebuzzini in [13], and it establishes a correspondence between accelerator modes of the physical system, and periodic orbits of the classical map

$$(5.1) \quad f: \begin{pmatrix} J \\ \theta \end{pmatrix} \mapsto \begin{pmatrix} J + \tilde{k} \sin(\theta + J) + \Omega \\ \theta + J \end{pmatrix} \pmod{2\pi}$$

where the J coordinate corresponds to the particles momentum, and θ to its coordinate. This map is of shear type, and the acceleration for a periodic orbit with rotation number q/p is given by

$$(5.2) \quad \alpha = \frac{2\pi q}{p} - \Omega$$

Hence, by analyzing the structure of existence of periodic orbits for the classical map above, we would be able to find which modes should be expected for which values of the parameters k and Ω . We remark that actual experimental observation also requires stability of the periodic orbits. It is important to stress here that since these parameters correspond to the kick strength and the time interval between kicks they can be controlled in the experiments as we wish, so results obtained for this system can be tested experimentally. When one plots the numerical results describing which periods exist for different values of k and Ω one gets an extremely complicated figure, see Figure 22.

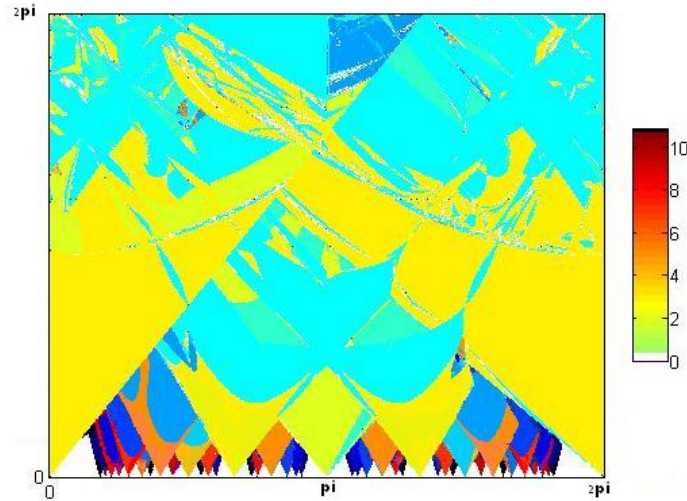


FIGURE 22. Tongues of periodic orbits.

An exact mathematical analysis of this system is extremely complicated. Perturbative methods have been used in [13] to analyze the existence of these “tongues” of periodic orbits in the region where $k \rightarrow 0$, as well as giving estimates on their widths.

Look at the map f given by (5.1) in regions where Ω is equal $(q/p)2\pi$ for some rational number q/p in the unit interval, and small k . For a small enough k it can be seen both from the numerical results shown graphically in Figure 22 and from perturbative arguments that in the above region a periodic orbit with period p exists.

For small k the periodic points of this orbit must be pretty much equally spaced along the J axis, and we can choose (for k small enough) a family of vertical loops that are equally spaced at distance exactly Ω apart, and each is at distance at least, say, $3k$ from any of the periodic points.

The image of a loop parameterized by $\Gamma_1(\theta) = \begin{pmatrix} J_0 \\ \theta \end{pmatrix}$ is given by

$$\begin{pmatrix} J_0 + k\sin(J_0 + \theta) + \Omega \\ J_0 + \theta \end{pmatrix} = \begin{pmatrix} J_0 + k\sin(\theta') + \Omega \\ \theta' \end{pmatrix}$$

and so is very close (for small k) to another loop of the chosen family. It follows that there exists a map \tilde{f} isotopic to f rel the orbit which keeps this family of curves invariant, and so, by Lemma 2.5, all the periodic orbits seen in the tips of the tongues in Figure 22 are simple orbits.

Note the rotation number of each of these orbits is equal exactly to the value of Ω in the tip of the tongue ($k = 0$) as for very small k the J coordinate

increases by an almost fixed value, close as we wish to Ω . And, by equation (5.2) the rotation number q/p is related to the acceleration of the corresponding acceleration mode by

$$\alpha = \frac{q}{p}2\pi - \Omega$$

So the topological meaningful numbers here are in fact also the ones with physical significance. While Ω changes through the region in which this periodic orbit exists, q/p is of course a topological invariant and therefore fixed. Hence the acceleration vanishes on the line with fixed Ω in the middle of each tongue, and changes signs when one crosses this line. This was measured experimentally in [15].

For any other point higher in the tongue which we can reach by an isotopy along which the periodic orbit exists, we also have the orbit is a simple orbit. We will assume, as is very natural and was checked numerically for many cases, that the orbits remain simple throughout the region of each tongue.

In some of the cases for which we drew a portrait of the phase space, we found that the fact the homeomorphism is isotopic to one which is reducible relative to the periodic orbit is realized by the physical map itself, as seen in Figure 23.

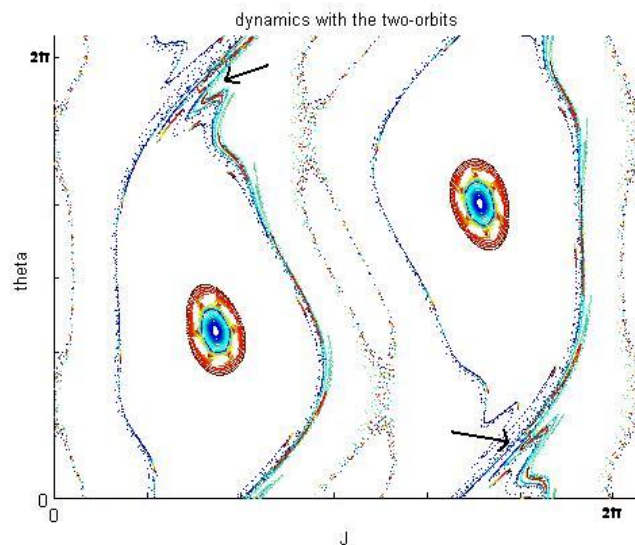


FIGURE 23. Phase portrait for a two-orbit. Drawn for $k = 2\pi/15$ and $\Omega = \pi$, the two-orbit which is clearly seen is a stable orbit with two stable neighbourhoods drawn. There is another two-orbit present, at which the arrows point, and it is the stable and unstable manifolds for this unstable orbit which divide the phase space into non intersecting regions which do not mix

Here the phase space is truly divided into pieces. Each of the annuli in this decomposition is mapped to another, and returns to itself with one twist after p iterations of f . Therefore every periodic orbit must have a period which is a multiple of p . On the other hand, when an annulus is mapped to itself with one twist under an area preserving map (here under f^p), every rotation number in the unit interval exists for it (here we mean the standard annulus rotation number measuring the rotations around the annulus), and so every period exists, as for every rational number n/m there is a periodic point of order m which rotates n times around the annulus before it returns to itself. This yields that for such a point in the parameter space, exactly all periods that are multiples of p exist. It is our belief that this situation is typical for the center of each tongue, that is for $\Omega = 2\pi q/p$. At other points, namely in all point we have numerically checked outside the center of the tongue, orbits of coprime lengths may exist simultaneously. We believe that the coexisting orbits whose rotation numbers are Farey neighbours form a simple pair together, as in the example on Figure 24, which shows a simple pair of orbits with rotation numbers $1/3$ and $1/2$ found in the physical system.

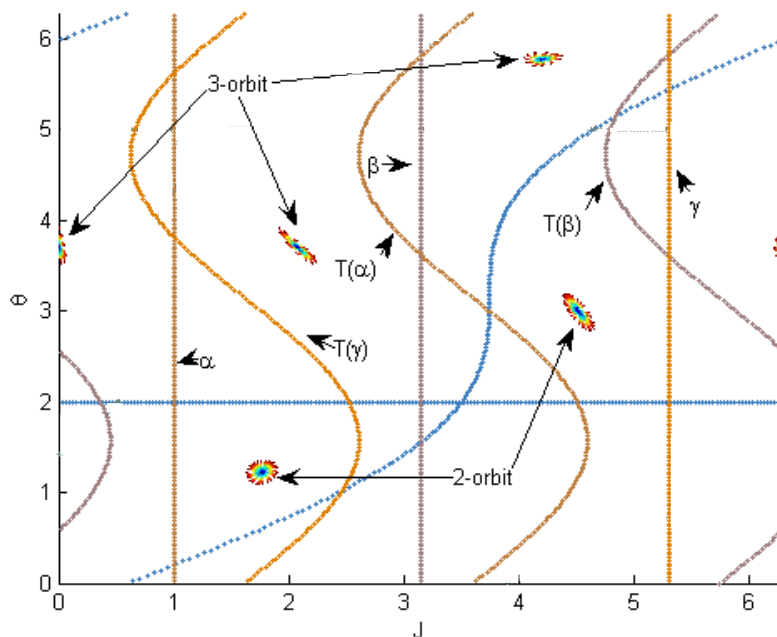


FIGURE 24. A pair of coexisting orbits in the physical system. Drawn with a collection of curves on the torus and their images, which show this is a simple pair.

This coexistence happens at a point in Figure 22 for which two tongues intersect. We assume that the same orbit persists throughout the tongue, and therefore we have at such a point two coexisting simple orbits. We believe that in all points of intersecting tongues coming from $k = 0$ and $\Omega_1 = q_1/p_1$, $\Omega_2 = q_2/p_2$ which are Farey neighbours, $p_1 > p_2$, the coexisting orbits form a simple pair.

Theorem 3.7 therefore implies that there are infinitely many periodic orbits for the parameters at a region of intersection of two such tongues, with rotation numbers equal to all rational numbers between the ones of these two tongues. If we assume all these simple orbits present also come from tongues, this yields that each rational tongue between q_1/p_1 and q_2/p_2 intersects each of these two tongues lower (along the k axis) than they intersect each other. In other words, following a path from a tip of a tongue upwards in the tongue, if it intersects a Farey neighbour tongue we know it intersects earlier all tongues of rational numbers between them. This determines the global structure appearing in Figure 22 of all accelerator modes in the physical system, as Sharkovskii's theorem determines it for one dimensional systems.

REFERENCES

- [1] R.L. ADLER, *Symbolic dynamics and Markov partitions*, Bull. Amer. Math. Soc **35** N1 (1998), 1-56.
- [2] D. ASIMOV AND J. FRANKS, *Unremovable closed orbits*, Geometric Dynamics, Lecture Notes in Mathematics, vol. 1007, 1983, pp. 22–29.
- [3] M. BESTVINA AND M. HANDEL, *Train-tracks for surface homeomorphisms*, Topology **34** (1992), 109–140.
- [4] P. BOYLAND, *Hamiltonian Dynamical Systems*, Contemp. Math., vol. 81, 1988, pp. 119–133.
- [5] ———, *Topological methods in surface dynamics*, Topology Appl. **58** (1994), 223–298.
- [6] ———, *Isotopy stability for dynamics on surfaces*, Geometry and Topology in Dynamics, Contemp. Math., vol. 246, 1999, pp. 17–45.
- [7] A.J. CASSON AND S.A. BLEILER, *Automorphisms of Surfaces after Nielsen and Thurston*, Cambridge University Press, 1988.
- [8] M.B. D'ARCY, G.S. SUMMY, S. FISHMAN AND I. GUARNERI, *Novel quantum chaotic dynamics in cold atoms*, Phys. Scripta **69** (2004), 25–31.
- [9] E. DOEFF, *Rotation measures for homeomorphisms of the torus homotopic to a Dehn twist*, Ergodic Theory Dynam. Systems **17** (1997), 1–17.
- [10] E. DOEFF AND M. MISIUREWICZ, *Shear rotation numbers*, Nonlinearity **10** (1997), 1755–1762.
- [11] T. HALL, *Unremovable periodic orbits of homeomorphisms*, Math. Proc. Cambridge Philos. Soc. **110** (1991), 523–531.
- [12] G.H. HARDY AND E.M. WRIGHT, *An Introduction to the Theory of Numbers*, Clarendon Press, Oxford, 1979.
- [13] S. FISHMAN, I. GUARNERI AND L. REBUZZINI, *Arnol'd tongues and quantum accelerator modes*, J. Statist. Phys. **110** (2003), 911; Phys. Rev. Lett. **89** (2002), 84101-1-4; Nonlinearity, submitted for publication.

- [14] M. MISIUREWICZ, *Rotation theory*, Online Proceedings of the RIMS Workshop on “Dynamical Systems and Applications: Recent Progress”.
- [15] Z.-Y. MA, M.B. D’ARCY AND S. GARDINER, *Gravity-sensitive quantum dynamics in cold atoms*, Phys. Rev. Lett. **93** (2004), 164101-1-4.
- [16] T. MATSUOKA, *Braids of periodic points and a 2-dimensional analogue of Sharkovskii’s ordering*, World Sci. Adv. Ser. in Dynamical Systems **1** (1986), 58–72.
- [17] M.K. OBERTHALER, R.M. GODUN, M.B. D’ARCY, G.S. SUMMY AND K. BURNETT, Phys. Rev. Lett. **83** (1999), 4447–4451.

Manuscript received October 25, 2010

TALI PINSKY
Department of Mathematics
The Technion
32000 Haifa, ISRAEL
E-mail address: otali@tx.technion.ac.il

BRONISŁAW WAJNRYB
Department of Mathematics
Rzeszów University of Technology
Powstańców Warszawy 6
35-959 Rzeszów, POLAND
E-mail address: dwajnryb@prz.edu.pl